INSULATOR-INSULATOR AND INSULATOR-CONDUCTOR TRANSITIONS IN THE PHASE DIAGRAM OF ALUMINIUM TRICHLORIDE

ROMINA RUBERTO,[a] GIORGIO PASTORE,[b*] AND MARIO P. TOSI [c]

ABSTRACT. We report a classical computer-simulation study of the phase diagram of $AlCl_3$ in the pressure-temperature *(p, T)* plane, showing (i) that melting from a layered crystal structure occurs into a molecular liquid at low *(p, T)* and into a dissociated ionic liquid at high *(p, T)*, and (ii) that a broad transition from a molecular insulator to an ionic conductor takes place in the liquid state.

1. Introduction

It was first proposed in an early x-ray diffraction study of liquid $AlCl_3$ near the standard freezing point (sfp) that this material melts from a layer structure with sixfold coordination of the Al ions into a liquid of molecular Al_2Cl_6 dimers formed by two edge-sharing tetrahedra [1]. Neutron diffraction experiments have verified the fourfold coordination of the Al ions in the melt near the sfp [2] and the values of the macroscopic transport coefficients and melting parameters confirm melting into a molecular liquid [3]. A similar melting mechanism seems to be operating in $FeCl_3$ at the sfp [4] (for a review on liquid trihalides see [5]). Very recently an x-ray diffraction study of $AlCl_3$ under pressure has reported what appears to be a sharp change in the slope of the melting curve $p_m(T)$ and has attributed it to a structural change of the melt from a molecular-network structure to an ionic-like structure [6]. It thus appears that an insulator-conductor transition may be taking place in this classical liquid under pressure. Transitions from insulating to conducting states have drawn much attention in cases where a substantial role is played by the valence electrons, a prototypic example being molecular dissociation and pressure ionization under isochoric heating in molecular hydrogen [7]. Other instances of insulator-conductor transitions in which valence electrons play the crucial role are met in Rb and Cs near the liquid-vapor critical point [8] and in solutions of metals in molten salts under changes in composition [9].

In this work we report on a study of the phase diagram of $AlCl_3$ over a wide portion of the pressure-temperature *(p, T)* plane, as obtained in classical molecular-dynamics simulations of its ionic structure and ionic diffusive motions. We describe this system by means

of a pseudoclassical interionic-force model that we have previously developed [10] to evaluate the liquid structure of this system near the sfp in comparison with that of other well known molecular trihalides ($AlBr_3$, $GaBr_3$ and GaI_3) and with neutron diffraction data on their total liquid structure factors [2, 11]. The model simulates the effects of chemical bonding between the ions in an isolated molecular unit by means of saturating electrical dipoles induced on the halogen ions [12] and accounts at a good quantitative level for the main observed features of the liquid structure at the sfp: fourfold coordination of the trivalent ions and stability of their first-neighbor shell, formation of intermediate-range order in addition to density and charge short-range order, metal-halogen and halogen-halogen bond lengths. Such a degree of success in describing a molecular liquid in terms of interactions between the individual ions (rather than in terms of interactions between permanent molecular units, as is commonly done in theoretical studies of molecular liquids) has induced us to extend our work to the study of the model as brought to extreme thermodynamic conditions far removed from the sfp [13], where the dimeric molecular units that are the main constituents of the liquid near the sfp are broken into monomers and ultimately crushed into their separately moving ionic constituents.

The contents of the present paper are as follows. In Section 2 we give for the first time a full display of the calculated phase diagram of $AlCl_3$ and of the calculated insulator-conductor transition line in the liquid state. We discuss the main features of this diagram and its comparison with the data reported by Brazkhin et al. [6]. We also report snapshots of the simulation sample in the liquid and layered-crystal states. All supporting material for our main result is collected in Section 3: the interionic-force law and the computer simulation method, the calculation of the pressure, the evolution of the statistical distribution of ion clusters on squeezing along high-temperature isotherms as structural evidence for the liquid-liquid transition, and the time-dependent mean-square displacements of the two ionic species as dynamical evidence for the liquid-liquid and liquid-solid transitions under isothermal squeezing. Finally, Section 4 ends the paper with a brief summary and some concluding remarks.

2. Phase diagram

Figure 1 reports our results for the phase diagram of our model simulating $AlCl_3$. The various symbols indicate simulation runs taken along different paths in the *(p, T)* plane. Starting from the bottom lozenge which is located at the sfp, we have followed both an isochoric heating path (lozenges) and an "isodiffusive" path (squares) along which the average of the diffusion coefficients of the two species is maintained as nearly as possible constant. Along the other paths, denoted by filled triangles, we have moved on high-temperature isotherms. Snapshots of the simulation sample in its three different states are shown in Fig. 2.

We proceed to describe the behaviors of the statistical distribution of cluster sizes along these paths. Here we geometrically define a cluster in the liquid as a group of ions such that all the Al-Cl neighbor distances are lower than 0.3 nm, this distance being in the middle of a range of Al-Cl bond lengths where at the sfp the Al-Cl pair distribution function is zero and the Al-Cl running coordination number is equal to four [10]. With this definition we find that at the sfp the Al_2Cl_6 dimers are the dominant cluster population, accompanied
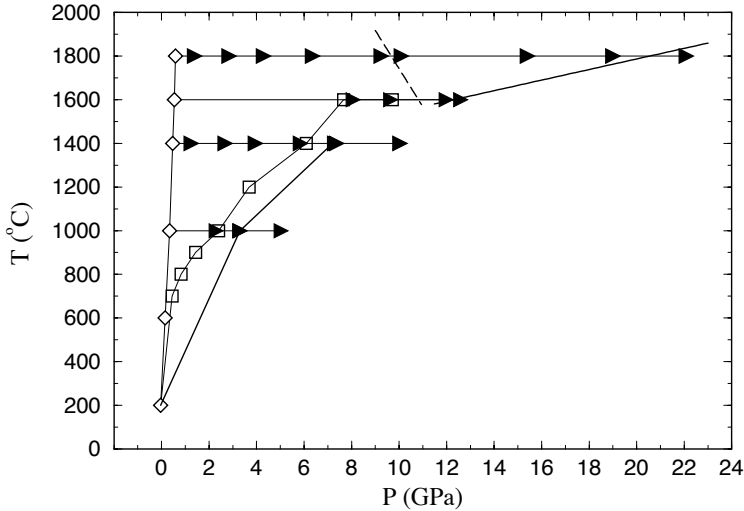
FIGURE 1. Map of the thermodynamic states studied by simulation in the temperature-pressure plane (see text); the thin full lines are guides to the eye) and proposed locations of the melting curve (heavy full lines) and of the liquid-liquid transition (heavy dashed line).

by some trimers and by very low numbers of higher n-mers up to hexamers. On raising the temperature of the sample up to 1800 °C along the sfp isochore, we find that these clusters tend to dissolve in favor of a growing population of monomers, which become the majority species at the highest temperature [13]. The energy needed to break a dimer into two monomers is estimated as $E \simeq 1$ eV, so that we expect that the dissociation process should set in at $T \simeq 1000$ °C according to the empirical rule [14] that a thermally activated excitation process in a classical system can occur when the thermal energy is of the order of 1/10 – 1/20 of a characteristic binding energy. Detachment of an ion from a monomer requires instead an activation energy of several eV and should therefore occur at much higher temperatures. There is indeed no trace that ionization is as yet occurring along the sfp isochore and we can already conclude that compression is needed for the onset of a molecular-to-ionic liquid-liquid transition in this temperature range.

We indeed meet the insulator-conductor transition in the liquid state by moving from the sfp along the isodiffusive path, along which we have to increase the pressure in order to maintain approximately constant the average diffusivity as temperature is raised. As we shall demonstrate in the next Section, the transition is signalled by two main features in the simulation sample: (i) the cluster population changes over from a majority of small clusters to formation of a single cluster comprising all the ions in the sample; and (ii) the diffusion coefficient of Al becomes larger than that of Cl, thus showing that the trivalent ions are becoming free to escape from their coordination shell. For obvious reasons we do not reach solidification of the sample along such an isodiffusive path, on which equilibration of the sample is becoming increasingly difficult.
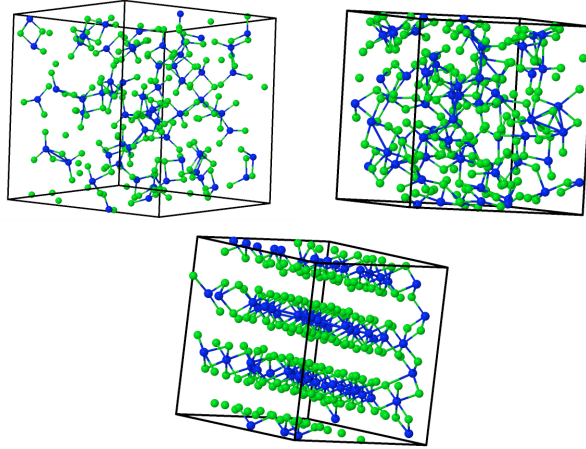
Figure 2. Snapshots of the structure of the simulation sample from the sfp (top left) to the ionic-liquid state at 1800 °C (top right) and to the layered-crystal state at 1800 °C (bottom).

We turn to discuss the behaviors of the sample along the isothermal paths indicated in Fig. 1. Along the lowest isotherm at 1000 °C we find that a liquid of dimers, accompanied by some monomers and trimers, directly solidifies under compression into a layered crystal structure containing a number of lattice defects. As can be seen from the bottom snapshot in Fig. 2, each layer of the crystal consists of two planes of Cl ions sandwiching a plane of Al ions in sixfold coordination sites: this is indeed the observed crystal structure of the real $AlCl_3$ material [15]. We meet the same behavior on the isotherm at 1400 °C , but at 1600 °C solidification is preceded by the insulator-conductor liquid-liquid transition, lying at the same pressure as we met it by moving along the isodiffusive path. Thus, at this temperature solidification occurs from a dissociated ionic liquid rather than from a molecular liquid. Finally, at 1800 °C the liquid-liquid transition is met at lower pressure and solidification occurs at higher pressure: the pressure range of stability for the ionic-liquid state is rapidly broadening. We show in Fig. 1 a schematic phase diagram in which we have joined by two heavy full lines the points where we estimate from our data that solidification occurs, and by a heavy dashed line the approximate location of the liquid-liquid ionization transition. We should stress that the latter transition is not a sharp one, but is spread out as we shall illustrate in the next Section. We may nevertheless try to use the Clausius-Clapeyron equation to interpret this transition line. We see from Fig. 1 that the molecular-to-ionic transition line has a negative slope, that we interpret as reflecting an increase of entropy and a decrease of specific volume across the transition. It has indeed been pointed out in earlier work [3] that a number of trihalides having solid-state structures composed from separate molecular units and melting into molecular liquids ($AlBr_3$, AlI_3, $GaCl_3$, $SbCl_3$ and $SbBr_3$) show a deficit in the entropy of melting relative to the norm for all other trihalides. One may thus expect that this deficit is made up in the ionization transition.

A negative sign for the volume change in the ionization transition is clearly consistent with our earlier remark that this transition at the temperatures of present interest is driven by pressure. It is also clear from Fig. 1 that the slope of our estimated melting curve is decreasing in the *(p, T)* range where solidification is a molecular-molecular (insulator-insulator) transition and becomes even smaller in the *(p, T)* range where solidification is an ionic-molecular (conductor-insulator) transition. Both entropy and volume changes can be expected to be negative in solidification. The Al-Cl running coordination number in the ionic-liquid state varies very slowly around a value six in the neighborhood of an Al-Cl distance of 0.3 nm [13], so that the coordination of the trivalent ions is approximately the same in this liquid as in the layered solid. One may surmise that in this situation melting involves a relatively low entropy change. As a final remark, we notice that the qualitative shape of the calculated melting curve that we have indicated in Fig. 1 resembles that obtained by Brazhkin et al. [6] from their x-ray diffraction data. These authors locate the change in melting regime of the layered $AlCl_3$ crystal, from melting into a molecular network to melting into an ionic structure, at approximately 1300 °C and 4 GPa. There is, therefore, a rough quantitative correspondence between our model predictions and their experiments.

3. Supporting material

We describe in this Section the main aspects of the calculations leading to the results shown in Figs. 1 and 2.

3.1. Interionic force law and simulation procedure. Our model for the interionic force law embodies the leading terms in a double expansion of the potential energy of the system into multipoles and into overlap integrals, as was originally proposed for the alkali halide monomers [16, 17]. At lowest order the potential energy depends only on the bond vectors $\mathbf{r}_{ij}$ between all ion pairs and contains the Coulomb interaction energy between the nominal ionic charges, the s-type Born-Mayer overlap repulsive energy, and a saturating van der Waals interaction between the halogens. At the next order the formation of dipoles $\mathbf{p}_h$, due both to electrical induction and to changes in the interionic overlaps, is allowed for the halogens. This implies that the component of a dipole along a first-neighbor bond length decreases and may even reverse sign as the bond length becomes short in the course of the ionic motions. As already noted, the values of the various force-law parameters are taken from an analysis of the structure of isolated monomers and dimers [12].

With the potential energy of the ionic assembly written as a function $U(\{ \mathbf{r}_{ij} \},\{ \mathbf{p}_h \})$ of all bond vectors and all dipoles on the halogens, we perform microcanonical molecular-dynamics runs based on Beeman's algorithm [18]. For each chosen thermodynamic state in the temperature-density plane we carry out a full implementation of Ewald sums for all long-range energy terms and determine by energy minimization at each time step of 2 fs the equilibrium values of the dipole moments, allowing full control on the accuracy in the evaluation of energy and forces. The details of the simulation protocol regarding initialization and equilibration of the sample, the sample size dependence, and the collection of statistics on various sample properties can be found in Ref. [10]. The final step of each run is to pass from a point in the temperature-density plane to a state in the pressure-temperature plane. We use for this purpose the expressions given by Wilson et al. [19] for

the real-space and reciprocal-space contributions to the stress tensor to evaluate from the same potential-energy function the pressure on the sample corresponding to its density and temperature.

3.2. Evolution of cluster sizes under pressure. The evolution of the statistics of average cluster populations along a high-temperature isotherm gives a most clear signal of the liquid-liquid transition. This is illustrated in Fig. 3 for the isotherm at 1800 °C . The low-pressure populations at this temperature consist primarily of monomers and dimers, but at higher pressure two different types of populations start coexisting: one is still primarily composed of monomers and dimers, and the other consists of clusters having size close to that of the simulation sample. On further increases in pressure the former population type disappears and the latter acquires a single size equal to the sample size. Solidification is met on this isotherm at a much higher pressure and can be visually seen from snapshots of the sample as reported in Fig. 2. It is evident from Fig. 3 that far away from the melting curve the liquid-liquid transition is not at all sharp, but is spread out over a range of a few GPa.

The statistics of cluster populations shows similar features on the isotherm at 1600 °C , although here the range of stability of the conducting state is much narrower as already remarked. On the isotherm at 1400 °C , on the other hand, the locations of the molecular-to-ionic transition and the solidification transition coincide, as far as we can tell from our simulations: that is, on this isotherm we do not meet a conducting state of the system and solidification has become a transition from a liquid insulator to a solid insulator, rather than a transition from a liquid conductor to a solid insulator. We interpret the difference in behaviors that we have found along the 1600 °C and 1400 °C isotherms as reflecting the presence of an intermediate anomaly on the melting curve, as reported from the experiments of Brazhkin et al. [6].

3.3. Evolution of ionic diffusivities under pressure. A clear dynamical signals of the liquid-liquid transition also comes from our simulations of the velocity autocorrelation (vac) functions of the two ionic species and from the related mean-square ionic displacements as functions of time. The vac spectrum in the molecular liquid state at low temperature contains a number of sharp peaks that can be related to the vibrational spectrum of isolated molecular units [13]. In the conducting liquid state, instead, the vac spectrum contains, in the frequency range that we can explore, just a single very broad hump as is typical of the ionic conductivity spectrum of a molten salt [20]. Figure 4 reports the mean-square displacements of the two ionic species as functions of time for various values of the pressure along the isotherm at 1800 °C. As is well known, the asymptotic slope of each curve is proportional to the ionic diffusion coefficient. In the molecular-liquid state the two species diffuse at very similar rates, with the diffusivity of the Cl ion being slightly larger than that of the Al ion. At the pressure of the liquid-liquid transition the two diffusivities become practically identical and in fact invert their order at still higher pressures in the ionic-conductor state. This mass-transport study confirms the results obtained from cluster sizes on the location of the liquid-liquid transition. A further signal comes from this study in regard to the solidification transition: we see from Fig. 4 that the diffusivities of both species essentially vanish at the highest pressure, where solidification has occurred.
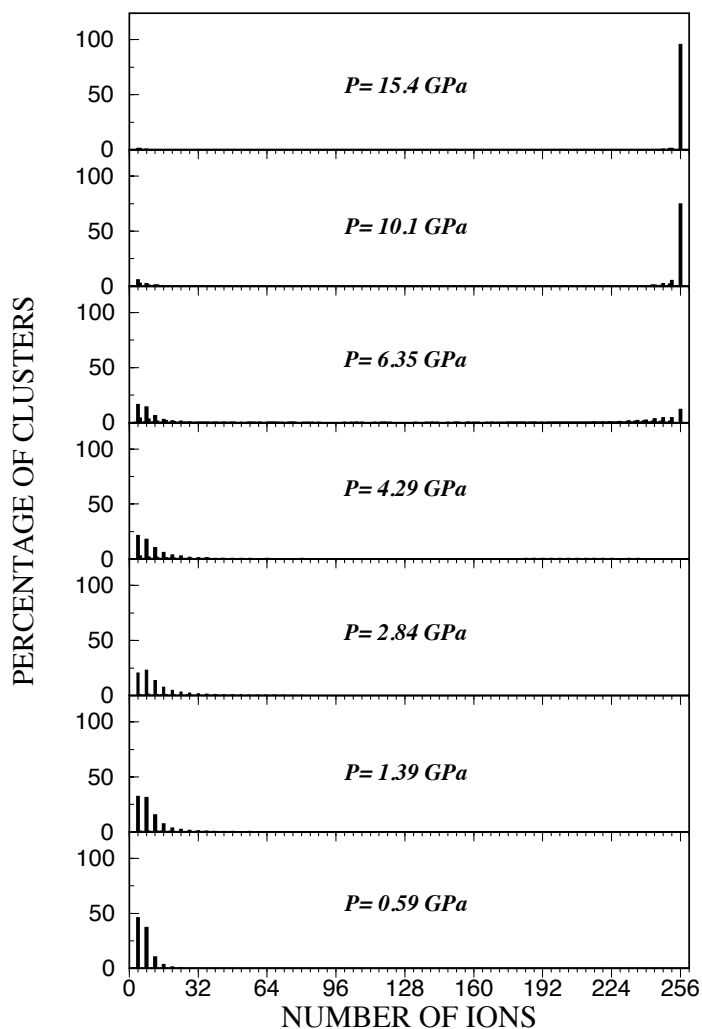
FIGURE 3. Histograms giving the population of various ion groups along the isotherm at 1800 °C at selected values of the pressure as indicated in each panel.

4. Summary and conclusive remarks

In summary, we have seen that a pseudoclassical computer-simulation model for $AlCl_3$ verifies the observed character of the melting curve as being a phase transition from a layered crystal into a molecular liquid at low pressure and temperature and into an ionic liquid at high pressure and temperature. We have also been able to trace the transition line between the two liquid states away from the melting curve, this liquid-liquid transition
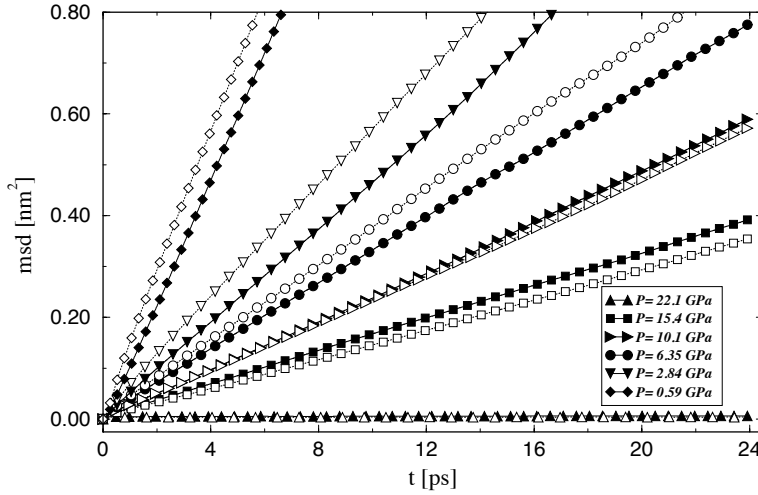
FIGURE 4. Mean-square displacements of the two ionic species (msd, in nm^2) as functions of time t (in picoseconds) at the sfp (top pair of curves) and with increasing pressure on the isotherm at 1800 °C up to solidification (bottom pair of curves). Open symbols refer to Cl and filled symbols to Al.

being driven by compression in the temperature range that we have investigated. The transition is most directly signaled in our study by the shape of the statistical distribution of ion clusters and by the crossing in the values of the diffusion coefficients of the two ionic species. Across this liquid-liquid transition the liquid undergoes gradual, though rapid, changes in structure, which are accompanied by increases in entropy and particle density. Direct breakage of molecular units under isochoric heating can only take place at much higher temperatures.

The x-ray diffraction study of Brazhkin et al. [6] has also reported that the melt of $ZnCl_2$ changes over from a molecular-network structure into an ionic structure with increasing pressure. A molecular-network structure can be obtained for this liquid in a pseudoclassical model on simply accounting for size and valence differences between the two ionic species, but conspicuous signals for a transition into an ionic conducting liquid are then harder to find in computer simulation runs. It also appears that an explicit account of covalency and relativistic effects may be needed in the theory of this material, as is suggested by the available theoretical studies of monomers and dimers of the related $HgCl_2$ compound [21].

Acknowledgments

References

[1] R. L. Harris, R. E. Wood and H. L. Ritter, "Title", *J. Amer. Chem. Soc.* **73**, 3150 (1951)

[2] Y. S. Badyal, D. A. Allen and R. A. Howe, *J. Phys.: Condens. Matteri* **6**, 10193 (1994)

[3] Z. Akdeniz and M. P. Tosi, *Proc. R. Soc. London* **A 437**, 85 (1992)

[4] Y. S. Badyal, M.-L. Saboungi, D. L. Price, D. R. Haeffner and S. D. Shastri, *Europhys. Lett.* **39**, 19 (1997)

[5] M. P. Tosi, D. L. Price and M.-L. Saboungi, *Ann. Revs. Phys. Chem.* **44**, 173 (1998)

[6] V. V. Brazhkin, A. G. Lyapin, S. V. Popova, Y. Katayama, H. Saitoh and W. Utsumi, *J. Phys.: Condens. Matter* **19**, 246104 (2007)

[7] W. R. Magro, D. M. Ceperley, C. Pierleoni and B. Bernu, *Phys. Rev. Lett.* **76**, 1240 (1996)

[8] R. Winter, W. C. Pilgrim and F. Hensel, *J. Phys.: Condens. Matter* **6**, A245 (1994)

[9] W. Freyland, K. Garbade and E. Pfeiffer, *Phys. Rev. Lett.* **51**, 1304 (1983)

[10] R. Ruberto, G. Pastore, Z. Akdeniz and M. P. Tosi, *Molec. Phys.* **105**, 2383 (2007)

[11] M.-L. Saboungi, M. A. Howe and D. l. Price, *Molec. Phys.* **79**, 847 (1993)

[12] Z. Akdeniz, G. Pastore and M. P. Tosi, *N. Cimento* **20**, 595 (1998)

[13] R. Ruberto, G. Pastore and M. P. Tosi, *Phys. Chem. Liq.* **46**, 548 (2008)

[14] N. H. March and M. P. Tosi, *Phys. Chem. Liq.* **10**, 39 (1980)

[15] R. W. G. Wyckoff, *Crystal Structures Vol. 2* (Interscience, New York, 1964)

[16] M. P. Tosi and M. Doyama, *Phys. Rev.* **151**, 642 (1966)

[17] P. Brumer and M. Karplus, *J. Chem. Phys.* **58**, 3903 (1973)

[18] M. P. Allen and D. J. Tildesley, *Computer Simulation of Liquids* (Oxford University Press, New York, 1987)

[19] M. Wilson, F. Hutchinson and P. A. Madden, *Phys. Rev. B* **65**, 094109 (2002)

[20] P. V. Giaquinta, M. Parrinello and M. P. Tosi, *Physica A* **92**, 185 (1978)

[21] M. Kaupp and H. G. von Schnering, *Inorg. Chem.* **33**, 2555 (1994)

[a]   Romina Ruberto
      Università degli Studi di Messina
      CNISM and
      Dipartimento di Fisica
      Contrada Papardo
      98166 Messina, Italy

[b]   Giorgio Pastore
      Università degli Studi di Trieste
      Dipartimento di Fisica Teorica and
      CNR-INFM DEMOCRITOS National Simulation Center
      Strada Costiera 11
      34100 Trieste, Italy
*   **E-mail**: pastore@ts.infn.it

[c]   Mario P. Tosi
      Scuola Normale Superiore
      Classe di Scienze and
      CNR-INFM-NEST
      Piazza dei Cavalieri 7
      56126 Pisa, Italy